Light trapping in horizontally aligned silicon microwire solar cells

Fredrik A. Martinsen,[1,*] **Benjamin K. Smeltzer,**[1] **John Ballato,**[2] **Thomas Hawkins,**[2] **Max Jones**[2] **and Ursula J. Gibson**[1]

[1]*Department of Physics, Norwegian University of Science and Technology, N-7491 Trondheim, Norway*

[2]*The Center for Optical Materials Science and Engineering Technologies (COMSET), School of Material Science and Engineering, Clemson, SC 29634, USA*

[*]*fredrik.martinsen@ntnu.no*

Abstract: In this study, we demonstrate a solar cell design based on horizontally aligned microwires fabricated from 99.98% pure silicon via the molten core fiber drawing method. A similar structure consisting of 50 μm diameter close packed wires (≈ 0.97 packing density) on a Lambertian white back-reflector showed 86 % absorption for incident light of wavelengths up to 850 nm. An array with a packing fraction of 0.35 showed an absorption of 58 % over the same range, demonstrating the potential for effective light trapping. Prototype solar cells were fabricated to demonstrate the concept. Horizontal wire cells offer several advantages as they can be flexible, and partially transparent, and absorb light efficiently over a wide range of incident angles.

OCIS codes: (160.6000) Semiconductor materials; (350.6050) Solar energy.

References and links

1. N. Guo, J. Wei, Q. Shu, Y. Jia, Z. Li, K.Zhang, H. Zhu, K. Wang, S. Song, Y. Xu, and D. Wu, "Fabrication of silicon microwire array for photovoltaic applications," Appl. Phys. A **102**, 109–114 (2011).
2. F.A. Martinsen, B. K. Smeltzer, M. Nord, T. Hawkins, J. Ballato, and U. J. Gibson, "Silicon-core glass fibes as microwire radial-junction solar cells," Sci. Rep. **4**, 6283 (2014).
3. M. Gharghi, E. Fathi, B. Kante, S. Sivoththaman, and X. Zhang, "Heterojunction Silicon Microwire Solar Cells," Nano Lett. **12**, 6278–6282 (2012).
4. H. P. Yoon, Y. A. Yuwen, C. E. Kendrick, G. D. Barber, N. J. Podraza, J. M. Redwing, T. E. Mallouk, C. R. Wronski, and T. S. Mayer, "Enhanced conversion efficiencies for pillar array solar cells fabricated from crystalline silicon with short minority carrier diffusion lengths," Appl. Phys. Lett. **96**, 213503 (2010).
5. M. D. Kelzenberg, D. B. Turner-Evans, M. C. Putnam, S. W. Boettcher, R. M. Briggs, R.M. Briggs, J.Y. Baek, N. S. Lewis, and H. A. Atwater, "High-performance Si microwire photovoltaics," Energy Environ. Sci. **4**, 866–871 (2011).
6. M. D. Kelzenberg, D. B. Turner-Evans, B. M. Kayes, M. A. Filler, M. C. Putnam, N. S. Lewis, and H. A. Atwater, "Photovoltaic measurements in single-nanowire silicon solar cells," Nano Lett. **8**, 710—714 (2008).
7. M. C. Putnam, S. W. Boettcher, M. D. Kelzenberg, D. B. Turner-Evans, J.M. Spurgeon, E. L Warren, R. M. Briggs, N. S. Lewis, and H. A. Atwater, "Si microwire-array solar cells," Energy Environ. Sci. **3**, 1037–1041 (2010).
8. D. R. Kim, C. H. Lee, P. M. Rao, I. S. Cho, and X. Zheng, "Hybrid Si microwire and plannar solar cells: passivation and characterization," Nano Lett. **11**, 2704–2708 (2011).
9. O. Gunawan and S. Guha, "Characteristics of vapor-liquid-solid grown silicon nanowire solar cells," Sol. Energy Mater. Sol. Cells **93**, 1388–1393 (2009).
10. B. Tian, X. Zheng, T. J. Kempa, Y. Fang, N. Yu, J. Huang, and C. M. Lieber, "Coaxial silicon nonowires as solar cells and nanoelectronic power sources," Nature **449**, 885–890 (2007).
11. R. He, T. D. Day, M. Krishnamurthi, J. R. Sparks, P. J. A. Sazio, V. Gopalan, and J.V. Badding, "Silicon p-i-n Junction Fibers," Adv. Mater. **25**, 1461–1467 (2013).

#241078 Received 19 May 2015; revised 8 Sep 2015; accepted 22 Sep 2015; published 8 Oct 2015

12. F. A. Martinsen, T. Hawkins, J. Ballato, and U. J. Gibson, "Bulk fabrication and properties of solar grade silicon microwires," APL Mat. **2**, 116108 (2014).
13. B. M. Kayes, H. A. Atwater, and N. S. Lewis, "Comparison of the device physics principles of planar and radial p-n junction nanorod solar cells," J. Appl. Phys. **97**, 114302 (2005).
14. M. D. Kelzenberg, S. W. Boettcher, J. A. Petykiewicz, D. B. Turner-Evans, M. C. Putnam, E. L. Warren, J. M. Spurgeon, R. M. Briggs, N. S. Lewis, and H. A. Atwater, "Enhanced absorption and carrier collection in Si wire array for photovoltaic application," Nat. Mater. **9**, 239–244 (2010).
15. J. Yoon, A. J. Baca, S. Park, P. Elvikis, J. B. Geddes, L. Li, R. H. Kim, J. Xiao, S. Wang, T. Kim, M. J. Motala, B. Y. Ahn, E. B. Duoss, J. A. Lewis, R. G. Nuzzo, P. M. Ferreira, Y. Huang, A. Rockett, and J. A. Rogers, "Ultrathin silicon solar microcells for semitransparent, mechanically flexible and microconcentrator module designs," Nature Mat. **7**, 907–915 (2008).
16. M. M. Adachi, M. P. Anantram, and K. S. Karim, "Core-shell silicon nanowire solar cells," Sci. Rep. **3**, 1546 (2013).
17. M.-H. Hsu, P. Yu, J.-H. Huang, C.-H. Chang, C.-W. Wu, Y.-C. Cheng, and C.-W. Chu, "Balanced carrier transport in organic solar cells employing embedded indium-tin-oxide nanoelectrodes," Appl. Phys. Lett. **98** 073308 (2011).
18. B. Ray, M. R. Khan, C. Black, and M. A. Alam, "Nanostructured electrodes for organic solar cells: analysis and design fundamentals," IEEE. J. Photovoltaics **3**, 318 (2012).
19. X. Zhang, C. W. Pinion, J. D. Christesen, C. J. Flynn, T. A. Celano, and J. F. Cahoon, "Horizontal silicon nanowires with radial p-n junctions: A platform for unconventional solar cells," J. Phys. Chem. Lett. **4**, 2002–2009 (2013).
20. E. F. Nordstrand, A. N. Dibbs, A. J. Eraker, and U. J. Gibson, "Alkaline oxide interface modifiers for silicon fiber production," Opt. Mater. Express **3**, 651–657 (2013).
21. J. Ballato, T. Hawkins, P. Foy, R. Stolen, B. Kokouz, M. Ellison, C. McMillen, J. Reppert, A. M. Rao, M. Daw, S. Sharma, R. Shori, O. Stafsudd, R. R. Rice, and D.R. Powers, "Silicon optical fiber," Opt. Express **16**, 18675 (2008).
22. B. L. Scott, K. Wang, and G. Pickrell, "Fabrication of n-Type Silicon Optical Fibers," IEEE Photonics Technol. Lett. **21**, 1798–1800 (2009).
23. C. Hou, X. Jia, L. Wei, S. Tan, X. Zhao, J. D. Joannopoulos, and Y. Fink, "Crystalline silicon core fibres from aluminium core preforms," Nat. Commun. **6**, 6248 (2015).
24. J. Gee, "The effect of parasitic absorption losses on light trapping in thin silicon solar cells," in 20th IEEE Photovoltaic Specialist Conference (PVSC) (IEEE, 1988), pp. 549–554.
25. T. H. Wang, E. Iwaniczko, M. R. Page, D. H. Levi, Y. Yan, H. M. Branz, and Q. Wang, "Effect of emitter deposition temperature on surface passivation in hot-wire chemical vapor deposited silicon heterojunction solar cells," Thin Solid Films **501**, 284–287 (2006).
26. V.A. Dao, J. Heo, H. Choi, Y. Kim, S. Park, S. Jung, N. Lakshminarayan, and Junsin Yi, "Simulation and study of the influence of the buffer intrinsic layer back-surface field, densities and interface defects, resistivity of p-type silicon substrate and transparent conductive oxide on heterojunction with intrinsic thin layer (HIT) solar cell," Sol. Energy **84**, 777–783 (2010).
27. M. Hilali, S. Saha, E. Onyegan, R. Rao, L. Mathew, and S. Banerjee, "Light trapping in ultrathin 25 micrometer exfoliated Si solar cells," Appl. Opt. **53**, 6140–6147 (2014).

1. Introduction

The continued interest in reducing the purity requirements, kerf losses and quantity of the base material for silicon solar cells has led to the investigation of a wide range of micro and nanostructured solar designs. One such design is the vertically aligned nanowire/microwire cell which has emerged as a promising candidate for achieving high conversion efficiencies at a low cost [1–8]. The majority of these solar cells consist of vertically aligned microwires with diameters D from ~ 1 μm up to ~ 30 μm. These are fabricated using vapor-liquid-solid growth ($D \sim 1$ μm) [5–7, 9, 10], deep reactive ion etching ($D \sim 10$ μm) [3, 4], high pressure chemical vapor deposition ($D \sim 10$ μm) [11], and molten core fiber drawing ($D \sim 30$ μm) [2, 12], and utilize a radial junction on the cylindrical surface of wires.

Two arguments are commonly used in favor of microwire radial junction devices. First, the design allows decoupling of the light incidence and carrier collection directions [13], and second, arrays of vertically aligned wires with a large aspect ratio can achieve a high absorption per unit volume of silicon [14]. The former argument implies that radial junction devices can be made from a low purity material with short minority carrier diffusion lengths, while the latter

#241078 Received 19 May 2015; revised 8 Sep 2015; accepted 22 Sep 2015; published 8 Oct 2015

implies the need for less silicon than conventional planar solar cells. For large diameter wires the collective area of the top surface becomes comparable to that of the sidewalls [2–4]. This surface then requires standard anti-reflection treatment in order to achieve high absorption and thus negates the light trapping advantages of the radial design. As it is favorable to fabricate radial junction solar cells from wires with a low surface to volume ratio and diameters comparable to the minority carrier diffusion length [13], alternative wire based solar configurations that can successfully utilize $\sim$ 10 μm diameter microwires with a radial junction while maintaining high light absorption are of interest.

Horizontal assemblies of ($>$10 μm) microwires can be used to make solar cells, similar to the μ-cell design [15], by fabricating radial junctions and placing electrodes along the length of the wires [Figs. 1(a) and 1(b)]. When made from wires produced in macroscopically long lengths, the radial junctions and the electrodes could be fabricated periodically along the length of the wires. While not realizing the increased surface area for charge collection [16–18] or resonant behavior [10] of nanowires, such a design would largely eliminate kerf and polishing losses, reducing the amount of silicon used compared with conventional wafer-based cells. Minority carrier extraction lengths will still be short, and if adequate light absorption is possible, this design has distinct advantages. The horizontal wire design was earlier proposed by Kelzenberg, *et al*. [14], and Zhang, *et al*. [19], but the small dimensions of the wires present contact-forming challenges and the diameter of the vapor-liquid-solid-grown wires impose a limitation in terms of low absorption values for single layers. The advent of larger diameter high pressure chemical vapor deposition structures and bulk quantities of molten core drawn wires overcomes this limitation, making it timely to re-evaluate the design.

Here we present a horizontally aligned silicon radial junction design based on microwires produced using the molten core fiber drawing method. The light trapping possibility of the structure has been assessed through simulations and experiments and the potential for realizing flexible and partially transparent solar cells has been investigated. Multi-wire assemblies have been fabricated and their performance has been evaluated through current-voltage and optical measurements. This proof-of-concept solar cell was not optimized, but demonstrates the light gathering principle, and a process that can lead to production of flexible solar cells from silicon formed directly from the melt into the shape needed for cell production.

2. The horizontal wire array

An example of the horizontal silicon microwire solar cell design is shown in Fig. 1(a) where wires are placed on a substrate with a spacing of 1.5 times the diameter of the wires. The contacts to the semiconductor-junction can be fabricated as shown in Fig. 1(b), where the dark region represents the p-type crystalline core and the lighter green region is an n-type emitter. In the case of a heterojunction, the emitter and base can be separated by thin intrinsic layer [inset in Fig. 1(b)]. For longer wires the electrode structure can be repeated with a periodicity determined by optimization of the device resistance, Auger recombination and other factors. For normally incident light on specular surfaces, some light will be lost to back reflection or transmission [Fig. 1(c)], depending on the nature of the substrate, making the cell performance and transparency dependent on the packing fraction of the wires. As an avenue for increasing the light absorption in opaque designs, the wires can be placed on a Lambertian reflector so that light passing between the wires can be intercepted by a wire after reflection. This geometry can be further optimized by embedding the structure in a transparent medium with a textured surface in order to scatter the light into the wires more efficiently [Fig. 1(d)].

Silica-clad silicon microwires were fabricated using the interface modifier described by Nordstrand, *et al*. [20], via the molten core fiber drawing method [2, 21–23] employing a conventional fiber tower. Bulk quantities of wires with a silicon core to silica clad outer diameter

#241078 Received 19 May 2015; revised 8 Sep 2015; accepted 22 Sep 2015; published 8 Oct 2015

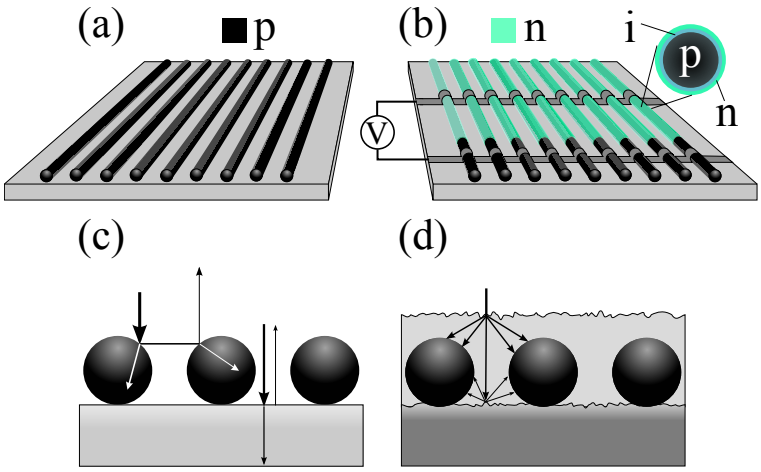

Fig. 1. Cell fabrication and light scattering: (a) microwires are placed in a horizontal array on a substrate, and (b) core-shell radial junctions and electrodes are fabricated along the length of the microwire. (c) The light trapping of the structure placed on a transparent substrate can be improved (d) by using a scattering top surface and by placing the wires on or above a Lambertian reflector.

ratio between 1:5-1:10 [Figs. 2(a) and 2(b)] were fabricated with core diameters between 10-200 μm [an exposed core is shown in Fig. 2(c)]. Microwires with sufficiently small diameter (typically $\lesssim$ 60-70 μm) are pliable as shown in Fig. 2(d) where a bend radius of $\approx$ 5 mm is demonstrated, suggesting the possibility of fabricating flexible solar cells from these materials.

3. Optical measurements and simulations

The optical absorption for the design was measured experimentally using assemblies of glass-coated silicon wires, as shown in Fig. 3(a), embedded in epoxy. The wires used to make these assemblies were made from solar grade n-doped silicon (ρ = 0.130-0.145 Ω cm) and had silicon core diameters measuring 50 μm $\pm$ 2 μm where the high uniformity originated from the wires all having been made in a single continuous draw. The assembled samples were mounted inside an integrating sphere and irradiated by light between 650-1100 nm with a bandwidth (FWHM) of approximately 50 nm at 750 nm. The portion of the light not absorbed by the structure − i.e. the reflected and transmitted components (R and T) − illuminated the sphere walls and was measured using a silicon detector mounted on a sphere port. The measured quantity $R+T$ was normalized to a Lambertian reference sample (Labsphere 6080 white reflectance coating on glass) with reflectivity between 95-98% over the measured spectral range, to account for any spurious losses. The sample absorption is thus approximately $1-R-T$. Samples for optical measurements were constructed by placing the glass-clad silicon wires adjacent to each other, with an average center-to-center distance (d), to make arrays larger than the 2 mm measurement beam. The packing fraction of silicon was varied by etching the glass cladding with HF acid for different amounts of time. This approach was chosen instead of fully stripping the cladding and subsequently assembling a structure as it allowed for increased accuracy in controlling the distance between the wires. The wires were embedded in an optically transparent epoxy (EPO-TEK® 301), which has a refractive index similar to silica. The absorption of the samples with various d-values was measured both with and without a Lambertian back-reflector (Labsphere 6080) for 0° and 45° incidence. For the samples measured without the back reflector the epoxy acted as the substrate as shown in Fig. 1(c).

#241078 Received 19 May 2015; revised 8 Sep 2015; accepted 22 Sep 2015; published 8 Oct 2015

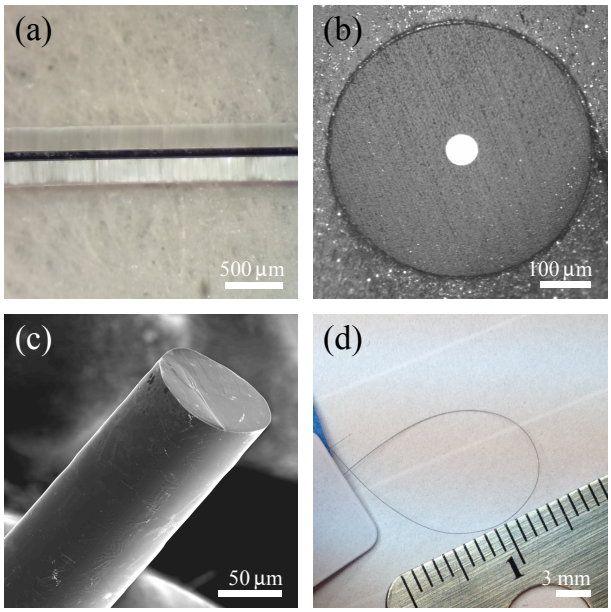

Fig. 2. Images of microwires produced using the molten core fiber drawing method. (a) An optical image of a large silica-silicon fiber (core appears magnified due to glass lensing), (b) a cross-sectional optical image of a similar fiber, (c) an SEM micrograph of a silicon core after glass removal, and (d) an image of a small-core fiber demonstrating a bending radius of ∼5 mm.

The sample absorption values $(1-R-T)$ at a center wavelength of 750 nm are shown in Fig. 3(b) as a function of wire packing fraction F (wire diameter/center-to-center distance d). At normal incidence, without the back-reflector, the absorption scales roughly linearly with packing fraction below $F = 0.2$ with a decreasing slope as F approaches unity. Adding the back-reflector, the absorption shows a similar trend but with an overall increase of about 10-15% absolute and an asymptotic behavior as F goes towards unity. This results in an absorption of $\approx 86\%$ for $F = 0.97$, while a reduction in F to 0.35 only reduced the absorption to $\approx 58\%$. The small reduction in absorption between $F = 0.97$ and $F = 0.35$ suggests efficient light trapping in our structures, compared to for example μ-cells, where the light absorption scales approximately linearly with packing fraction [15]. For an incidence angle of 45° without the back-reflector, a slight increase in absorption is seen over the normal incidence case, mainly because the array presents an effectively higher packing fraction. With the back-reflector in place, the light is more effectively coupled into the silicon even at normal incidence, and little change is seen when the incidence angle is changed. The measurements were repeatable to within ± 2 %, re-inserting and aligning the same sample. For the $F = 0.97$ case (fully-stripped wires) the ≈ 2 mm beam overfilled the sample at 45° incidence, thus this data point is omitted.

A self-consistent approach similar to that described by Gee [24] was used to model the performance of the wire arrays at 0° incidence as a function of F. The underlying assumptions are that there is randomization of the ray direction at the Lambertian reflector and silicon surfaces, and that total internal reflection occurs for those rays scattered into angles greater than the critical angle for the epoxy. This leads to light trapping. The array reflection and transmission coefficients shown in Fig. 3(c) were calculated using the optical constants of Si at 750 nm, assuming the wires were embedded in a medium of refractive index $n = 1.5$. Direct wire-to-wire coupling of light was neglected for simplicity, such that $R_{\text{array}} = R_{\text{Si}}F$, and $T_{\text{array}} = 1-F$,

#241078 Received 19 May 2015; revised 8 Sep 2015; accepted 22 Sep 2015; published 8 Oct 2015

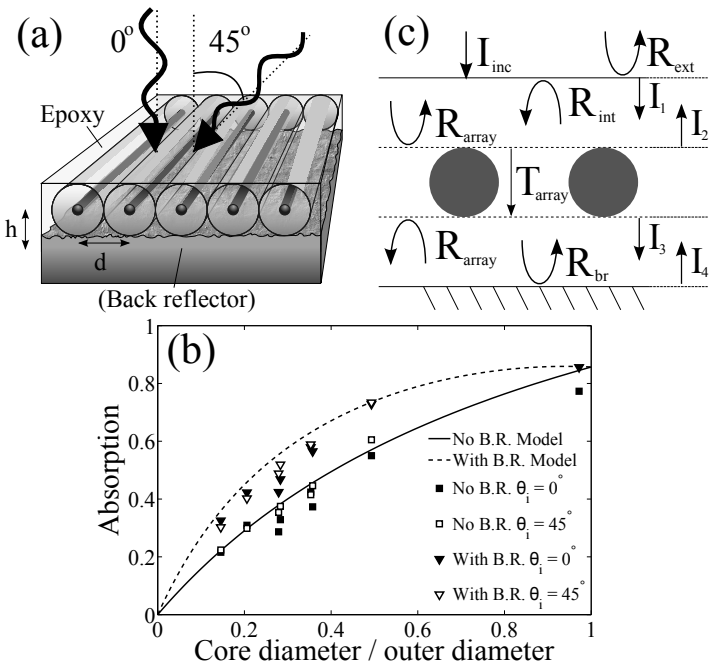

Fig. 3. (a) Schematic of the geometry used for measuring the absorption and (b) the corresponding absorption data measured for 0° and 45° incident light with and without a Lambertian back reflector. The absorption was modeled as shown schematically in (c), taking into account the various reflection and transmission terms in the samples.

where R_{Si} is the weighted angular average of Si reflectance. The reflectance of the outer epoxy-glass surface R_{ext} was assumed to be 4% and the internal surface reflectance $R_{\mathrm{int}} = 0.57$ was calculated assuming the reflected light from the silicon (and backreflector) is isotropic, following Gee [24]. The back-surface reflectance was 97% for the Lambertian coating, and 57% (R_{int}) without the back-reflector. As the structures are too large to give interference effects, the intensities I_{1-4} shown in Fig. 3 (c) can be expressed as:

$$I_1 = (1 - R_{\mathrm{ext}})I_{\mathrm{inc}} + R_{\mathrm{int}}I_2, \tag{1a}$$

$$I_2 = R_{\mathrm{array}}I_1 + T_{\mathrm{array}}I_4, \tag{1b}$$

$$I_3 = T_{\mathrm{array}}I_1 + R_{\mathrm{array}}I_4, \tag{1c}$$

$$I_4 = R_{\mathrm{br}}I_3. \tag{1d}$$

For the modeled wavelength of 750nm, the absorption length is $\sim$1 μm, so no light is transmitted through the wires, losses are purely reflective, and no diameter dependence is expected within the range of the wire sizes studied. In our model, we assume some randomization of the direction of the reflections, and the results are comparable to a slab of the same thickness, depending on the surface condition of the slab. The model does not account for inter-wire coupling, but in the case of the short wavelengths, these effects are expected to be negligible. The array absorption is $A_{\mathrm{array}} = (1 - R_{\mathrm{array}} - T_{\mathrm{array}})(I_1 + I_4)$, and this curve is plotted with and without a back-reflector in Fig. 3(b). The model reproduces the behavior of the experimental data without a backreflector, and provides a reasonable fit to the data with the Lambertian backreflector. The value used (0.97) for the Lambertian surface reflectance may be an overestimate since the reflector was characterized in air, but was covered by epoxy in the array measurements.

#241078 Received 19 May 2015; revised 8 Sep 2015; accepted 22 Sep 2015; published 8 Oct 2015

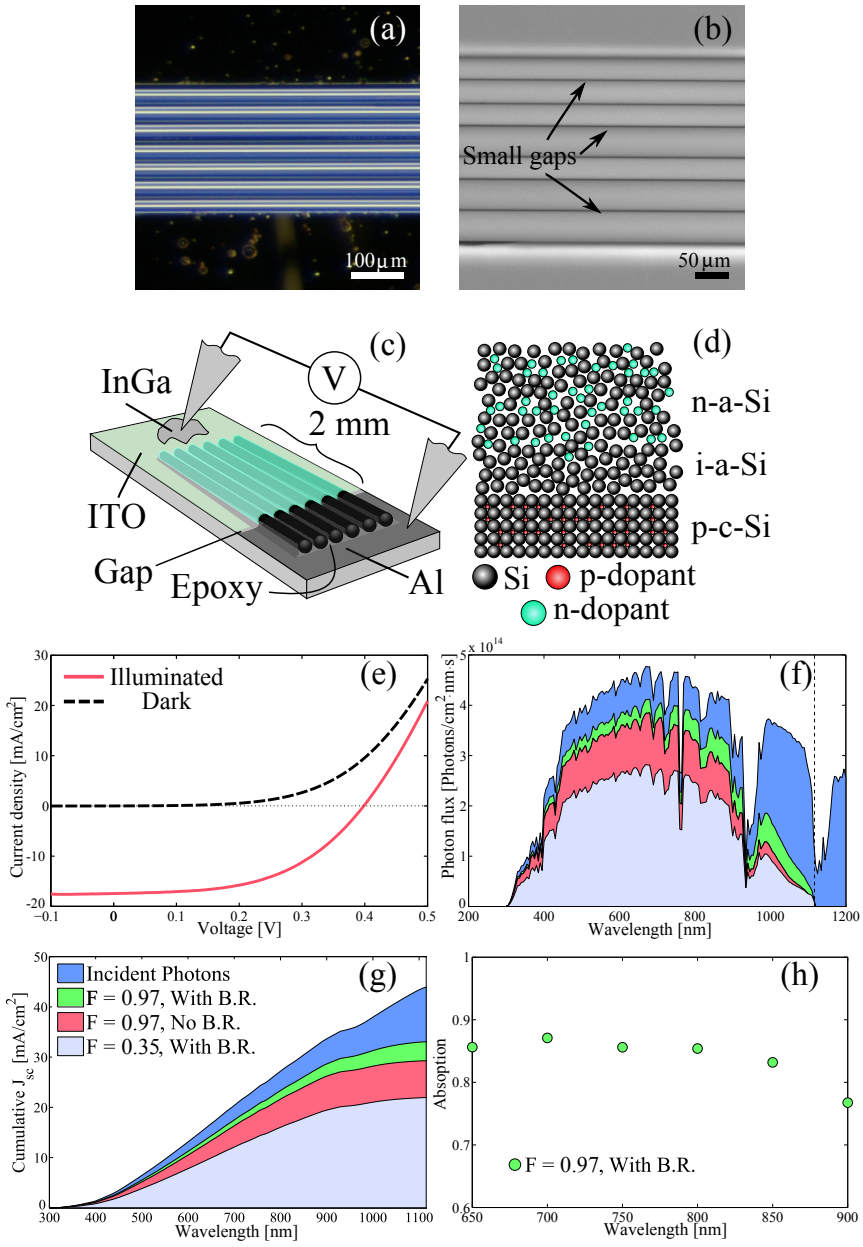

Fig. 4. (a) An optical image of a close packed fiber assembly of ∼35 µm diameter fibers and (b) a scanning electron micrograph of the core-shell part of a multi-fiber solar cell structure made from wires with ∼ 50 µm diameter. (c) Schematic of the full cell structure and (d) the junction formed by PECVD deposition of amorphous silicon. (e) I-V characteristics of a cell with an IQE ∼0.6 made from 6 wires with varying diameters similar to those in (b). The spectral absorption of an $F = 0.97$ and $F = 0.35$ sample are presented in (f); g) presents the upper bound on the current possible [IQE=1] for the absorption values shown in (f). The F= 0.97 array absorbs 67% of the relevant photons. The 0.97 fill factor is due to small gaps between the wire cores, illustrated in (b). (h) Details of spectral dependence of the absorption in the roll-off region (650 – 900 nm) for the F=0.97 sample.

#241078 Received 19 May 2015; revised 8 Sep 2015; accepted 22 Sep 2015; published 8 Oct 2015

This would lead to an overestimate of the absorption at low F, since I4 is a direct function of the back surface reflectance, and is more influential at low F.

4. Prototype solar cell

Prototype multi-wire solar cells $\approx$ 2 mm long, based on the intrinsic thin layer (HIT) design were fabricated from 6-8 wires with diameters of $\approx$ 50 μm [Figs. 4(a)–4(d)]. The wires used for making the prototype solar cells were made from p-type upgraded metallurgical silicon and originated from a series of different fiber draws giving them a diameter variation of $\sim$ 30%. The wires were the same as described in [12] and for more information the reader is referred to this publication. Wires fully stripped of their silica cladding were mounted with epoxy close packed ($\approx$ 0.97 packing density] on a silicon nitride coated glass substrate [Fig. 4(c)) and then cleaned using a piranha solution (3:1 H_2SO_4:H_2O_2) followed by 5% HF acid before the contact to the p-type core was applied through e-beam evaporation of 500 nm aluminum under a vacuum better than 10^{-7} torr. The piranha etch was kept short ($\sim$ 2 s) in order to clean the exposed parts of the wires, illustrated in Fig. 4(c), without over-etching the epoxy and removing the wires from the substrate. To fabricate the junction, the area of the wires contacted with aluminum was masked using photoresist followed by an HF acid dip (5 % HF) and subsequent deposition of $\approx$ 7 nm of intrinsic amorphous silicon, over-coated with $\approx$ 25 nm of phosphorous-doped amorphous silicon at 150° C [Figs. 4(c)–4(d)] using plasma enhanced chemical vapor deposition (PECVD). A relatively thick amorphous layer compared with that used in standard planar HIT-cells [25, 26] was applied to ensure full coating of the areas of the silicon surface close to the wire edges. The amorphous emitter was subsequently contacted using 80 nm of sputter deposited indium-tin oxide (ITO $\rho = 1.7 \cdot 10^{-3}$ Ω·cm) deposited in an 5 mTorr ambient consisting of 2% oxygen in argon at a substrate temperature of 100° C. Lift-off of the photoresist and ITO from the aluminum contact regions was then performed and the solar cells were measured at room temperature under AM 1.5G illumination using an indium-gallium eutectic for a contact to the ITO. The resulting I-V curves from the $\approx$ 2 mm long 6 wire champion cell taken under dark and illuminated conditions are shown in Fig. 4(e). Normalized to the illuminated area (cross sectional area of the cell), the cell showed a V_{oc} of 400 mV, a J_{sc} of 17.4 mA·cm^{-2} and a 0.51 fill factor, resulting in a 3.5% conversion efficiency. While the cells were fabricated on a rigid glass substrate, it is worth noting that the low temperature processes and pliable wires [Fig. 2(d)] are compatible with a polymer substrate. Extension of this fabrication method to formation of flexible solar cells may thus be possible.

5. Discussion

In the demonstrated solar device structure the wires were mounted close-packed onto a glass substrate using epoxy (illustrated schematically in Fig. 4(c)), resulting in the p-i-n-junction, and thus surface passivation, only being applied to approximately half of the wire surface. Earlier measurements of the recombination velocity on similar wires showed a reduction from $\sim$ 10000 cm·s^{-1} for non-passivated surfaces to $\sim$ 500 cm·s^{-1} for surfaces passivated with intrinsic amorphous silicon [12]. This is believed to be the main cause of the low observed V_{oc}. The fill factor of 0.51 is indicative of a high series resistance together with the presence of non-infinite shunt, with the former partly caused by the relatively resistant ITO layer ($\sim$ 1 Ω·cm^2 per mm) and the contact resistance (measured to $\approx$ 0.5 Ω·cm^2). With a wire resistivity of 0.3-0.9 Ω·cm [12], the series resistance contribution from the wires themselves is between 0.06 and 0.18 Ω·cm^2, and thus negligible compared with the other values in this device.

In order to interpret the observed J_{sc}, the absorption performance of the $F = 0.97$ structure, a similar but larger version of the structure presented in Fig. 3(b), was measured as a function of wavelength at 0° incidence without a Lambertian back reflector (red curve in Fig. 4(f)).

#241078 Received 19 May 2015; revised 8 Sep 2015; accepted 22 Sep 2015; published 8 Oct 2015

Extrapolated values of the absorption were used below 650 nm. Assuming a 100% internal quantum efficiency (IQE), the measured absorption was weighted by the solar spectral photon flux density in order to obtain the upper bound on the J_{sc} for this geometry. The resulting value for the cumulative J_{sc} as a function of wavelength is shown in Fig. 4(g). Based on the measured absorption, the calculated maximum J_{sc} for the $F = 0.97$ structure without a back-reflector was $\approx$ 29 mA·cm^{-2} (external quantum efficiency (EQE) of $\approx$ 67 %), a value comparable to that obtained for ultra-thin planar silicon wafers [27]. The measured value of 17.4 mA·cm^{-2}, which includes parasitic absorption of light in the ITO and amorphous layers, then gives a lower bound of 0.6 for the IQE in this prototype device.

A similar measurement performed with a back-reflector (assuming an IQE = 1) for $F = 0.35$ and $F = 0.97$ resulted in J_{sc}-limits of 22 mA·cm^{-2} and 33 mA·cm^{-2} respectively. These correspond to an EQE of 0.5 and 0.75 respectively, indicating that a reduction in silicon of $\approx$ 64 % only reduces the integrated light absorption by $\approx$ 33 %. Figure 4(f) shows that the single wavelength absorption values presented in Fig. 3(c) agree well with the spectral absorption up to around 850 nm [Fig. 4(h)], but from 850 nm to the band gap ($\approx$ 1100 nm) the absorption drops off for both configurations. The addition of an anti-reflective coating, together with improved randomization of the light inside the structure from more Lambertian-like front and back surfaces, or the introduction of scattering centers in the host matrix may be expected to further increase the overall light absorption of the structure.

The size of the prototype fabricated was limited by the availability of stripped microwire cores, but was adequate to demonstrate the fabrication principle. Scale-up could potentially be realized by employment of filament winding equipment used for layup of fiber-glass-reinforced materials or other textile equipment.

6. Conclusion

In conclusion we have shown that horizontally aligned silicon microwires produced via the molten core fiber drawing method have the potential to be employed as viable solar cells. The efficiency of the presented prototype was low due to the lack of process optimization, with surface recombination and series resistance believed to be the main limiting factors. However, the close packed array was shown to absorb $\approx$ 86 % of the light for wavelengths up to about 850 nm while a reduction of the packing fraction to 0.35 only reduced this absorption to 58 %. The horizontal structure shows similar absorption both for 0° and 45° incidence, suggesting that the light absorption in this design is largely independent of the incident angle.

Acknowledgments

This work was financially supported by the Norwegian Research Council, the Norwegian Micro- and Nano-Fabrication Facility, NorFab (197411/V30), and the NTNU Discovery Program.

#241078 Received 19 May 2015; revised 8 Sep 2015; accepted 22 Sep 2015; published 8 Oct 2015